JOURNAL OF COLLOID AND INTERFACE SCIENCE 173, 500–514 (1995)

The Adsorption of Dioxan by Porous Carbons

COLIN H. ROCHESTER[1] AND ALISTAIR STRACHAN

Chemistry Department, The University, Dundee DD1 4HN, United Kingdom

Received October 24, 1994; accepted January 11, 1995

Four carbon samples were characterized by nitrogen adsorption as nonporous, mixed meso- and microporous, largely microporous with some mesopores, and highly microporous. The general forms of isotherms for the adsorption of dioxan on the carbons resembled the results for nitrogen adsorption. The nonporous carbon constituted an acceptable standard material giving an average area occupied by adsorbed dioxan of 0.424 nm^2 and hence allowing estimation of surface areas of porous carbons which were consistent with corresponding areas deduced from the nitrogen adsorption data. Analysis of dioxan isotherms by the α_s-method gave effective micropore volumes and mesopore surface areas in broad agreement with corresponding results derived from nitrogen adsorption isotherms.

Key Words: dioxan adsorption; sorption by porous carbons.

INTRODUCTION

Gaining detailed information about the surface area and porosity of porous solids is a highly desirable objective (1). However, particular difficulties are encountered when trying to fully characterize an adsorbent of mixed porosity. Unfortunately many of the most important adsorbents comprise nonhomogeneous pore systems and, therefore, the need exists to devise methods which can be conveniently applied to such solids. Macropores may be insignificant contributors to adsorption on samples of mixed porosity and so attention may be primarily confined to studies of micropores, mesopores, and systems for which vapor adsorption exhibits characteristics of both these pore-size ranges. The adsorption of molecules of increasing size may lead to eventual exclusion from the pore structure as the ratio of adsorbate size to pore width is increased. This would provide a complete pore analysis if sufficiently large molecules could be employed to extend the method into the mesopore range. The incorporation of adsorption from solution into the analytical scheme provides the means to bridge the gap created by the limit in the size of readily vapourizable molecules.

The present study of the adsorption of dioxan vapor on four carbons with widely differing physical characteristics was intended as the first stage of investigation of the adsorption from solution of crown ethers on porous carbons. The main aims were to test similarities between the [illegible] of nitrogen (at 77 K) and dioxan (ca. 293 K) on [illegible] of different pore structure, to test the presence or absence specific sites for the adsorption of dioxan on typical [illegible] surfaces, and hence to assess to what extent the [illegible] of large crown ethers from solution might be influenced by adsorption on specific sites as well as steric factors [illegible] from inaccessibility of micropore surfaces. The values surface areas derived from nitrogen and dioxan [illegible] data are estimated from BET analyses (2) which would be unacceptable for anything other than comparative purposes (3) for solids containing a microporous component. Similarly the micropore analysis method (4) is used to compare micropore distributions in the present carbons although it is recognized that this method is based on the questionable assumption that multilayers form in micropores in the same way as on an open surface. However, more rigorous analyses (5–7) for carbons containing both micropores and mesopores go beyond the scope of the present comparative study. Micropore volumes and mesopore surface areas are [illegible] deduced from α_s-plots and also provide a comparison of [illegible] derived from nitrogen and dioxan adsorption isotherms.

EXPERIMENTAL

The four carbon samples were as follows: (a) AX21, petroleum pitch-based active carbon (Anderson Development Co.), also available as Amoco Carbon PX21 and prepared by heating petroleum coke with KOH (8), (b) CEC CXV, a pinewood-based steam-activated carbon, (c) M158H, a pinewood-based modified active carbon which has been subjected to high temperature heat treatment, and (d) Vulcan 3-G, graphitized carbon black (National Physical Laboratory) certified surface area reference material (71 m^2 g^{-1}).

Dioxan (BDH AnalaR, >99.5%) was purified by stirring overnight with 0.4 wt% $NaBH_4$ then adding CaH_2 and fractionating, before distillation from Na wire under dry nitrogen collecting the middle 80% fraction (9). The dioxan was freeze–thaw degassed before use in the adsorption experiments.

Nitrogen adsorption isotherms on the four carbons at 77 K were measured volumetrically using either a Carlo Erba

[1] To whom correspondence should be addressed.

0021-9797/95 $12.00

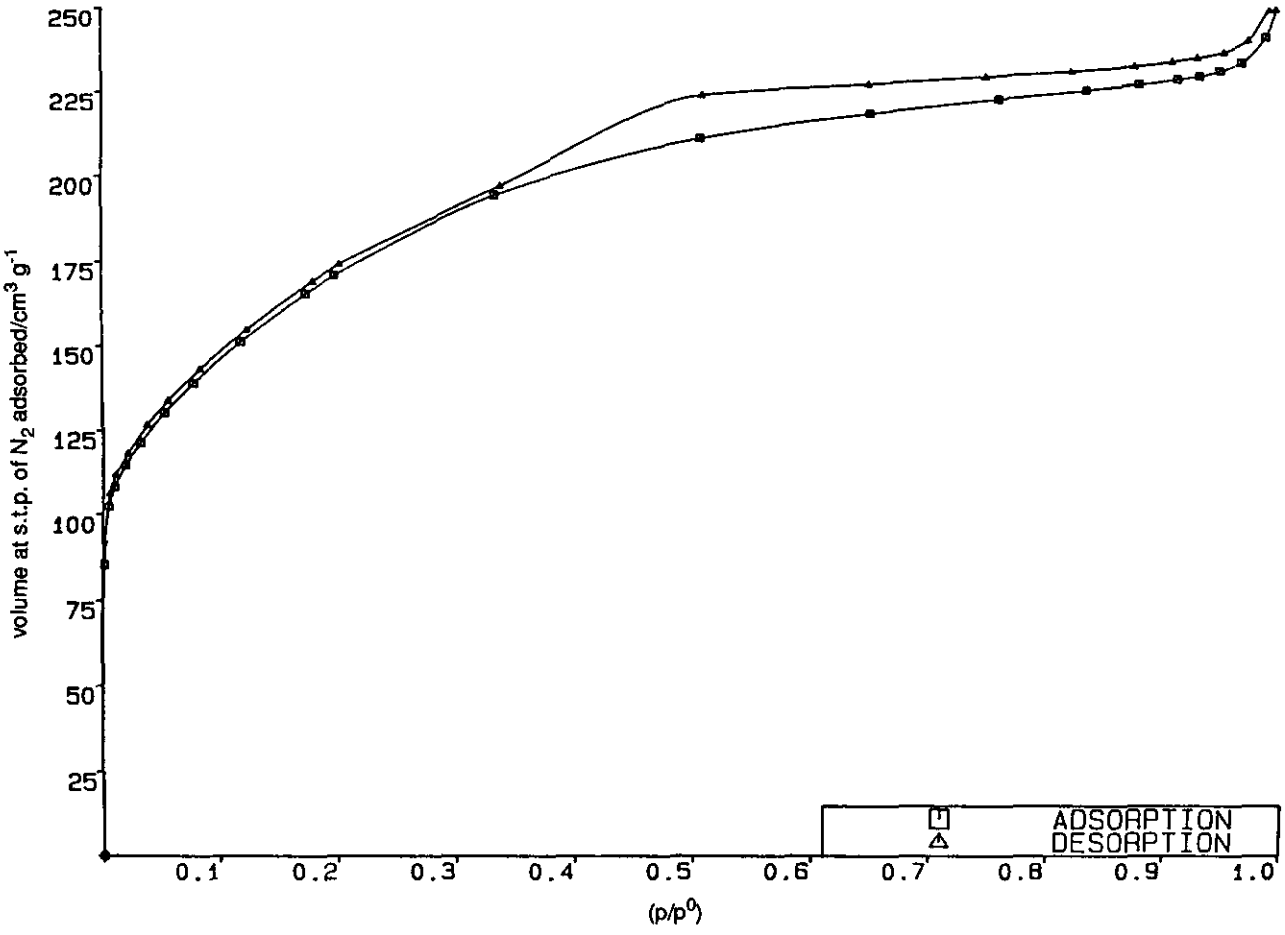

FIG. 1. Isotherm for N_2 on M158H at 77 K.

Series 1800 Sorptomatic or a Micromeritics ASAP 2400 instrument. Experiments with two different masses of each adsorbent confirmed the reproducibility of the results. Dioxan adsorption was studied gravimetrically using a CI Electronics 5-mg Mk2 vacuum balance head linked to a ROBAL digital control unit. Pressures were measured by transducers (Schaevitz types P702-0001 and P522-0001) which were linked together with the digital control unit and a thermocouple to a LINSEIS analogue printer which allowed easy recognition of the point at which equilibrium was attained for a given adsorption point. Unless otherwise stated BET plots were generally linear for p/p^0 up to ca. 0.15.

RESULTS AND DISCUSSION

Nitrogen Adsorption Isotherms

M158H. The carbon was heated at 573 K for ca. 16 h in vacuum (ca. 10^{-4} N m^{-2}) prior to nitrogen adsorption at 77 K. Volumes reduced to STP of nitrogen adsorbed per unit mass of outgassed carbon are given as a function of relative pressure in Fig. 1. Measurements took 5 h for adsorption and 9 h for desorption. The isotherm could be classified as type IV according to the BDDT system of Brunauer *et al.* (10). The usual interpretation is that the initial section can be attributed to monolayer–multilayer adsorption but the high uptake of N_2 at low relative pressure (ca. 50% of the adsorption capacity is taken up by $p/p^0 = 0.03$) causing a broad concave section suggests microporosity is present. Thus, the isotherm is probably more accurately described as type I + IV since it exhibits features typical of both. The broad knee suggests the presence of a range of micropore sizes which fill by both primary and secondary mechanisms. The hysteresis loop is best described (11) as type H4 and is most likely due to capillary condensation in narrow slit-like pores which are typical of active carbons. A BET (2) analysis of the isotherm data gives a monolayer capacity ν_m = 142 cm^3 g^{-1}, a c-parameter of 112, and a surface area A = 618 m^2 g^{-1}. The high value of c provides further evidence for the presence of microporosity. An estimate of micropore distribution has been gained from the micropore analysis method (4) which relies on the shape of t-plots (12–14). Analysis involving 24 pore groups gave a cumulative total volume of 0.318 cm^3 g^{-1} with ca. 80% of this total contained in the pore diameter range 0.8–1.3 nm. The narrowest pores appear to be ca. 0.66 nm diameter.

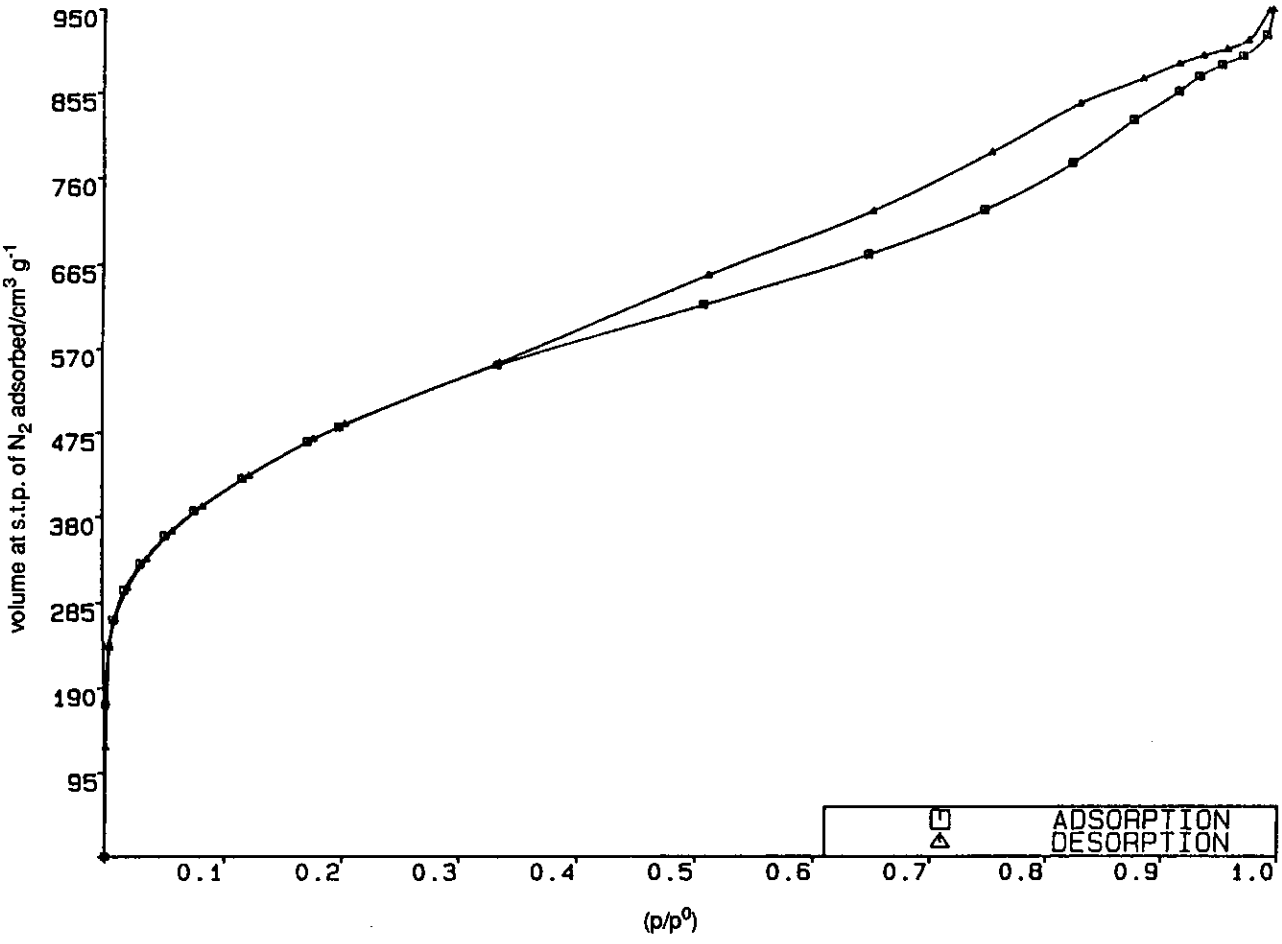

FIG. 2. Isotherm for N_2 on CECA CXV at 77 K.

CECA CXV. The isotherm for CECA CXV pretreated at 573 K (16 h, 10^{-4} N m^{-2}) was recorded over 12 h for adsorption and over 16 h for desorption and showed type I + IV mixed character (10) (Fig. 2) with the high uptake of N_2 at low relative pressure being indicative of microporosity. BET analysis (2) gave a c-value of 96, similar to that for M158H and a computed surface area of 1752 m^2 g^{-1}. The hysteresis loop is of type H3 (11) which suggests the possibility of capillary condensation being between open-ended slit-shaped pores. H3 loops are characteristic of mixed-pore systems and for CECA CXV, coupled with the broad high nature of the isotherm at lower pressures, this points to the presence of pores in both the micro and meso size ranges. The micropore analysis method (4) gave results similar to those for M158H with ca. 75% of the cumulative pore volume of 0.702 cm^3 g^{-1} in the diameter range 0.8–1.3 nm but with an enhanced number of pores up to 2.0 nm diameter. Again pores as low as 0.66 nm diameter were present.

AX21. The isotherm for AX 21 preheated at 573 K (16 h, 10^{-4} N m^{-2}) was of type I (10) (Fig. 3), which is characteristic of a microporous adsorbent. Adsorption took 9 h and desorption 18 h. The difference between the adsorption and desorption curves for $0.4 < (p/p^0) < 0.98$ is probably too small to be attributable to hysteresis. The high adsorption capacities 50% space filled at $(p/p^0) = 0.01$ and 90% filled at $(p/p^0) = 0.30$ confirm the highly microporous character of AX 21. The rounded concave knee over the low-pressure region of the isotherm $[(p/p^0) < 0.3]$ suggests that a range of micropore sizes were present. However, micropore analysis (4) showed that ca. 82% of the cumulative pore volume of 1.434 cm^3 g^{-1} was contained in a narrow band of pore widths in the range 0.8–1.0 nm with no pores <ca. 0.7 nm. The computed surface area of 3098 m^2 g^{-2} (c = 100) for AX 21 is of questionable significance.

Vulcan 3-G. After heat treatment at 573 K as for the other carbons, Vulcan 3-G gave a type II isotherm (10) which on BET analysis (2) gave a surface area of 72 m^2 g^{-1} in good agreement with the NPL value of 71.3 m^2 g^{-1}.

Dioxan Adsorption Isotherms

Vulcan 3-G. Dioxan on Vulcan 3-G gave a type II isotherm with no hysteresis (see Fig. 4). Vulcan 3-G was used as a nonporous reference solid for the carbon samples

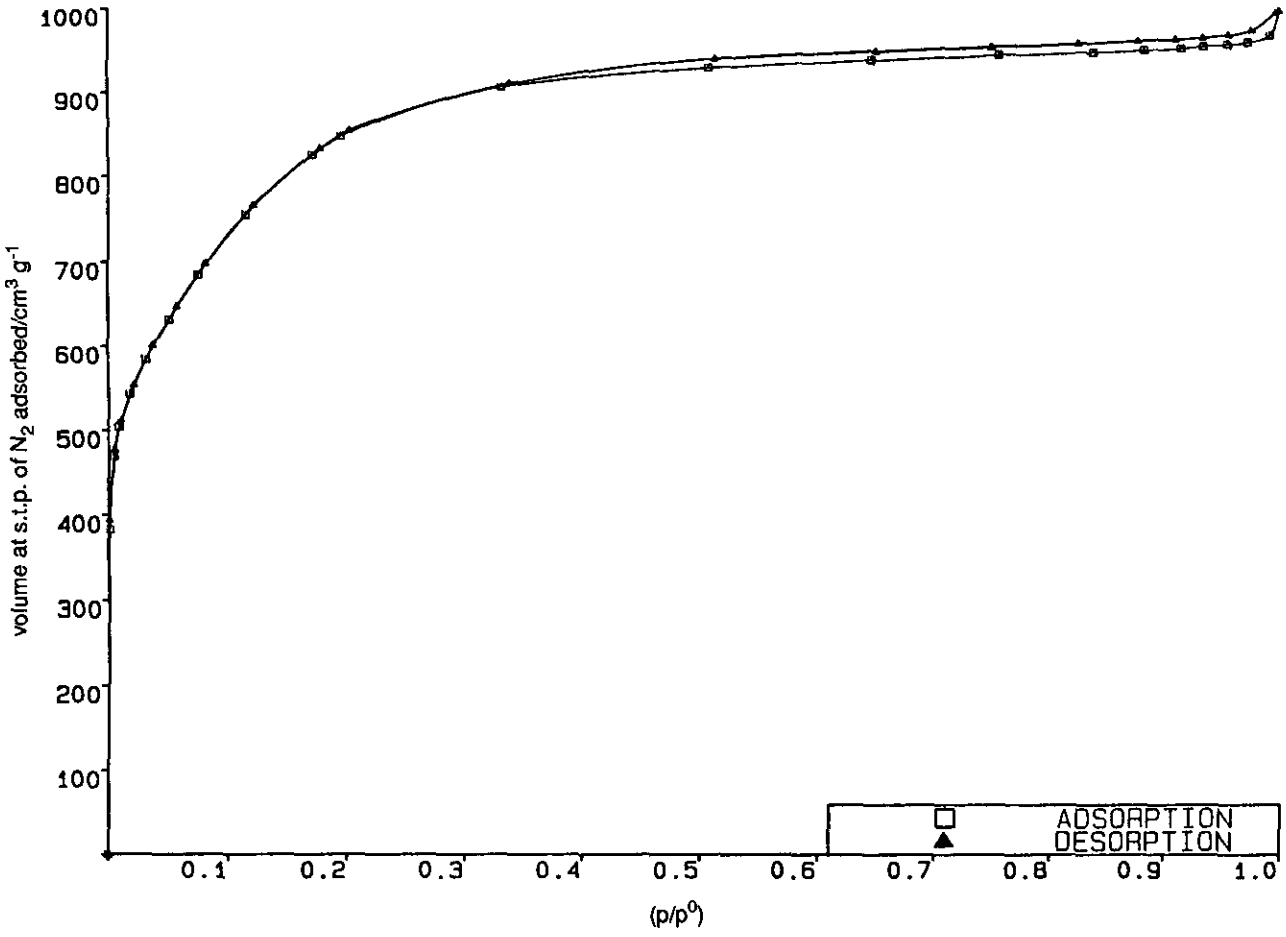

FIG. 3. Isotherm for N_2 on AX 21 at 77 K.

studied here and the area of carbon surface occupied per adsorbed dioxan molecule was based on the accurately known BET surface area of the reference. A BET plot for dioxan adsorption was linear in the range $0.05 < (p/p^0) < 0.3$ and gave a monolayer capacity in terms of mass per gram of adsorbent of 24.59 mg g^{-1} which corresponds, taking $A = 71.3$ m^2 g^{-1} for Vulcan 3-G, to an average area occupied per adsorbed dioxan molecule of 0.424 nm^2. The p^0 value for dioxan was calculated from the Antoine equation (15)

$$\log_{10}(p^0/\text{torr}) = 7.43155 - \frac{1554.679}{(t + 240.337)},$$

in which t is the temperature in °C.

M158H. The isotherm for dioxan adsorption on M158H (Fig. 5) showed, as for nitrogen adsorption, both type I and type IV character with marked hysteresis and a high uptake of dioxan at low pressures. However, the hysteresis differs from the nitrogen case because the loop is closed at $(p/p^0) > 0.7$ but persists to the lowest relative pressures studied. Nitrogen and dioxan adsorption uptakes on 158H have been converted to equivalent liquid volumes and plotted together for comparison (Fig. 6). Data used are dioxan liquid density = 1.0336 g cm^{-3}, nitrogen gas density = 1.25×10^{-3} g cm^{-3}, and nitrogen adsorbed phase density = 0.808 g cm^{-3}.

The saturation uptakes in Fig. 6 are similar, suggesting that the same pore space is available to both nitrogen and dioxan. The difference in shape between the isotherms can be accounted for by the larger size of the dioxan molecule. A larger adsorbate would normally interact with an adsorbent to a greater extent at a given relative pressure, causing an enhancement in adsorption. Figure 6 is consistent with this prediction for $(p/p^0) >$ ca. 0.02–0.05. However, the behavior appears reversed at very low relative pressures, where it might be expected that the enhancement in dioxan adsorption would be most pronounced. Consideration of the reasons for the low-pressure hysteresis exhibited by dioxan (Fig. 5) is helpful in this context.

Three possible causes of low-pressure hysteresis are the irreversible chemical interaction of the adsorbate with the adsorbent, the swelling of the adsorbent, and the irreversible uptake of adsorbate in pores or pore entrances of similar widths to the molecules themselves. The swelling phenome-

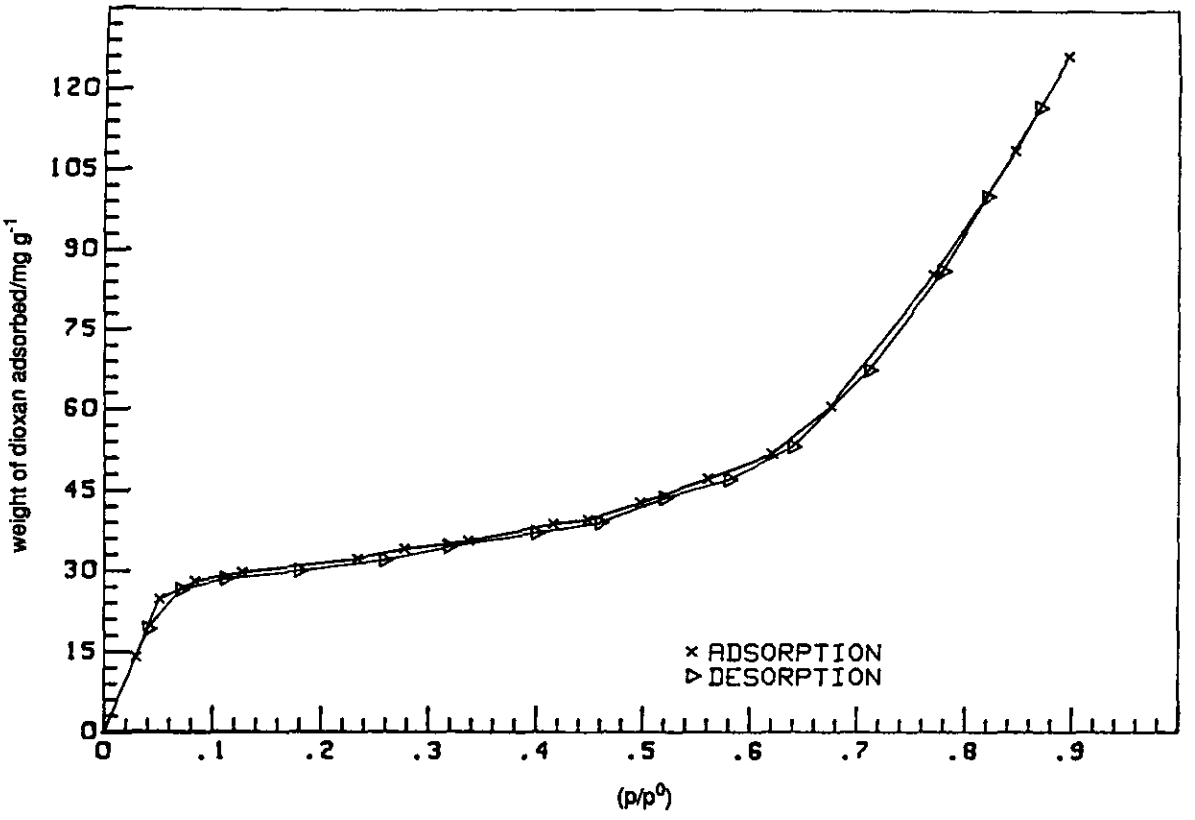

FIG. 4. Isotherm for dioxan on Vulcan 3-G at 293.2 K.

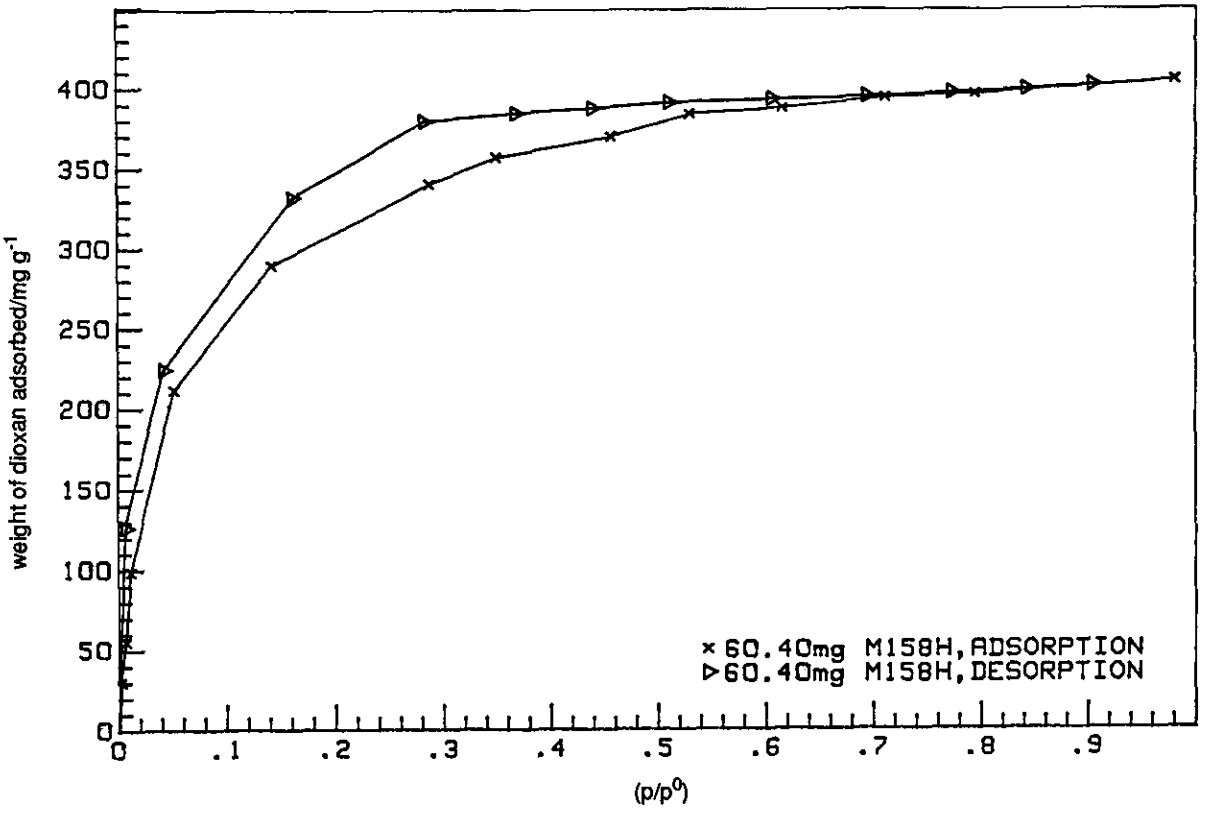

FIG. 5. Isotherm for dioxan on M158H at 293.0 K.

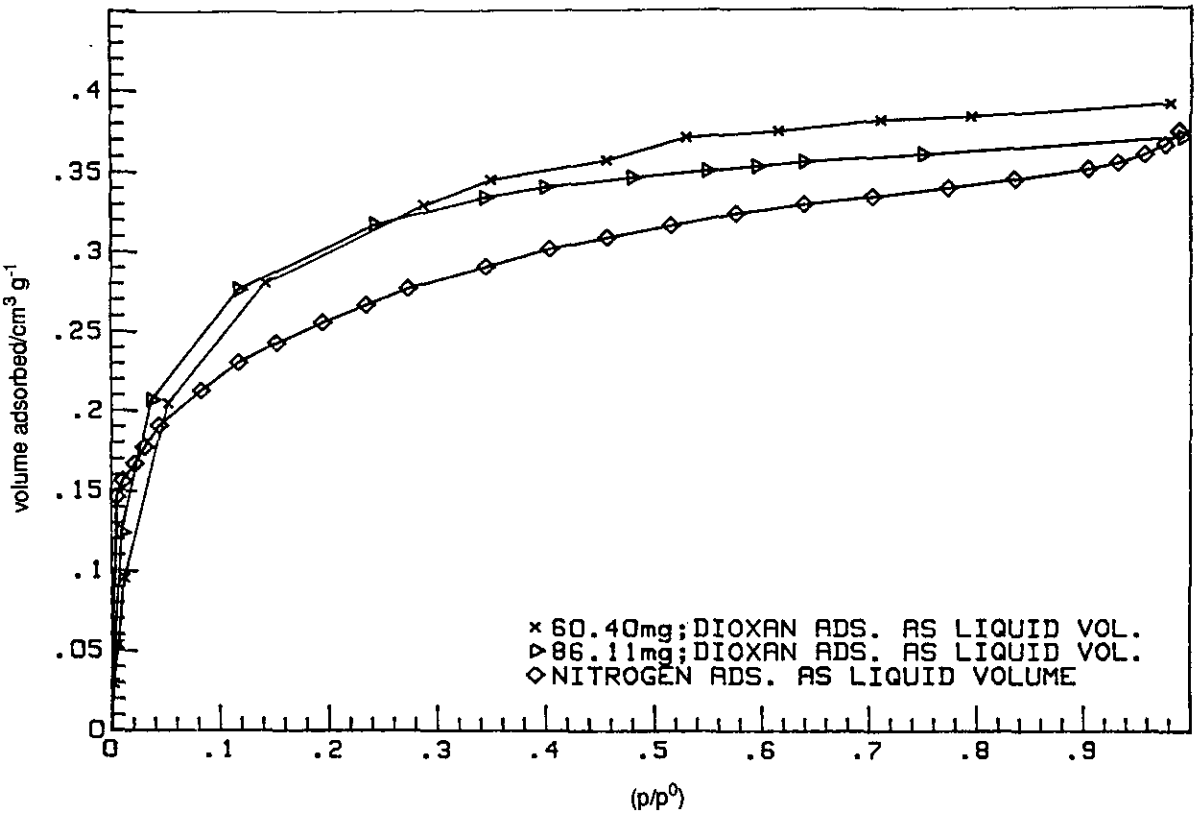

FIG. 6. Comparison of nitrogen and dioxan uptakes by M158H as liquid volumes.

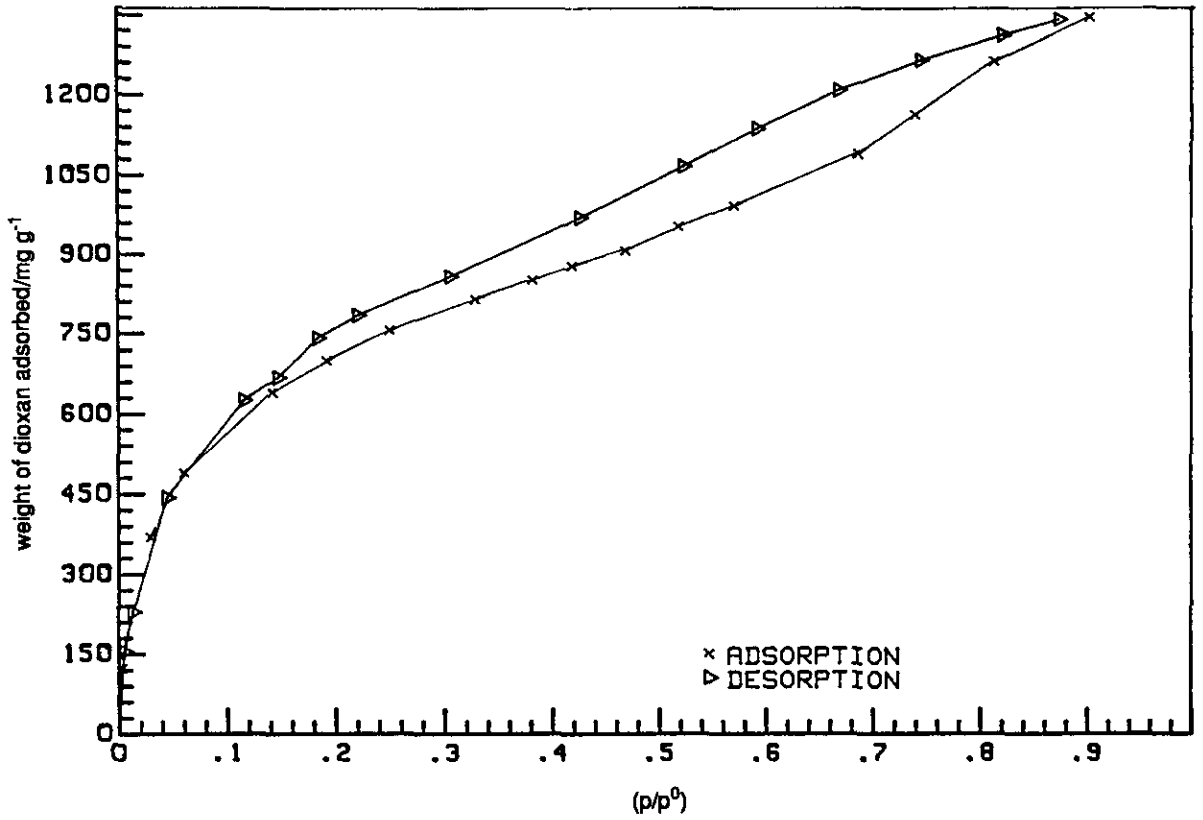

FIG. 7. Isotherm for dioxan on CECA CXV at 293.2 K.

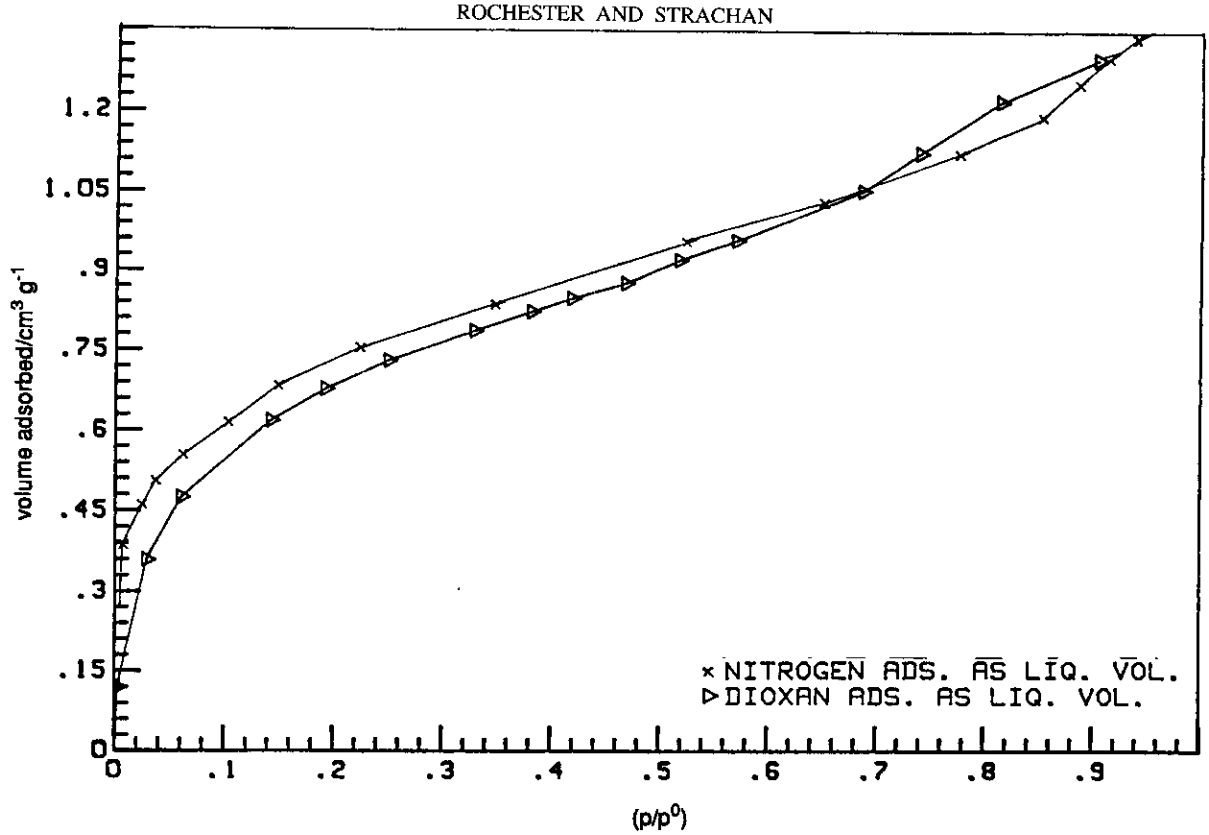

FIG. 8. Comparison of nitrogen and dioxan uptakes by CECA CXV as liquid volumes.

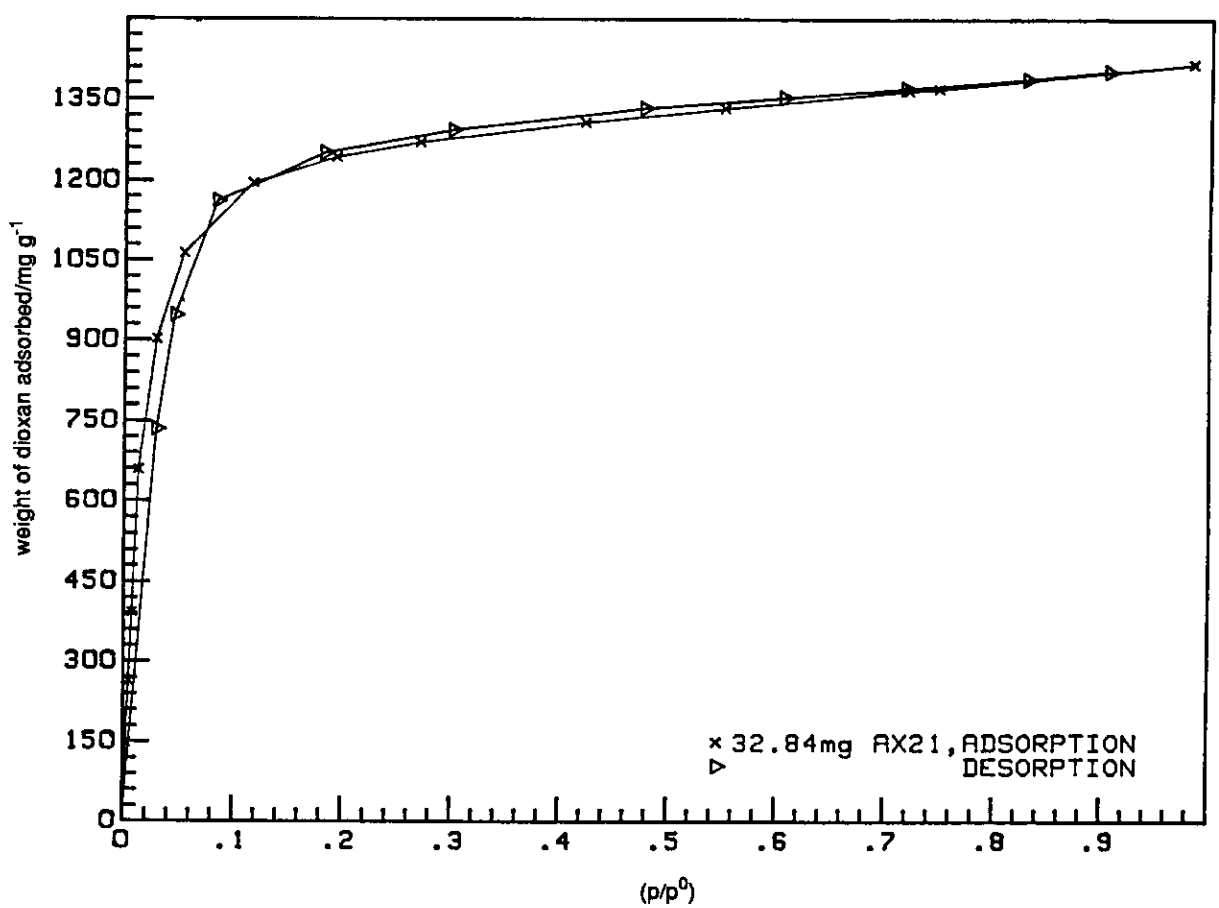

FIG. 9. Isotherm for dioxan on AX21 at 293.5 K.

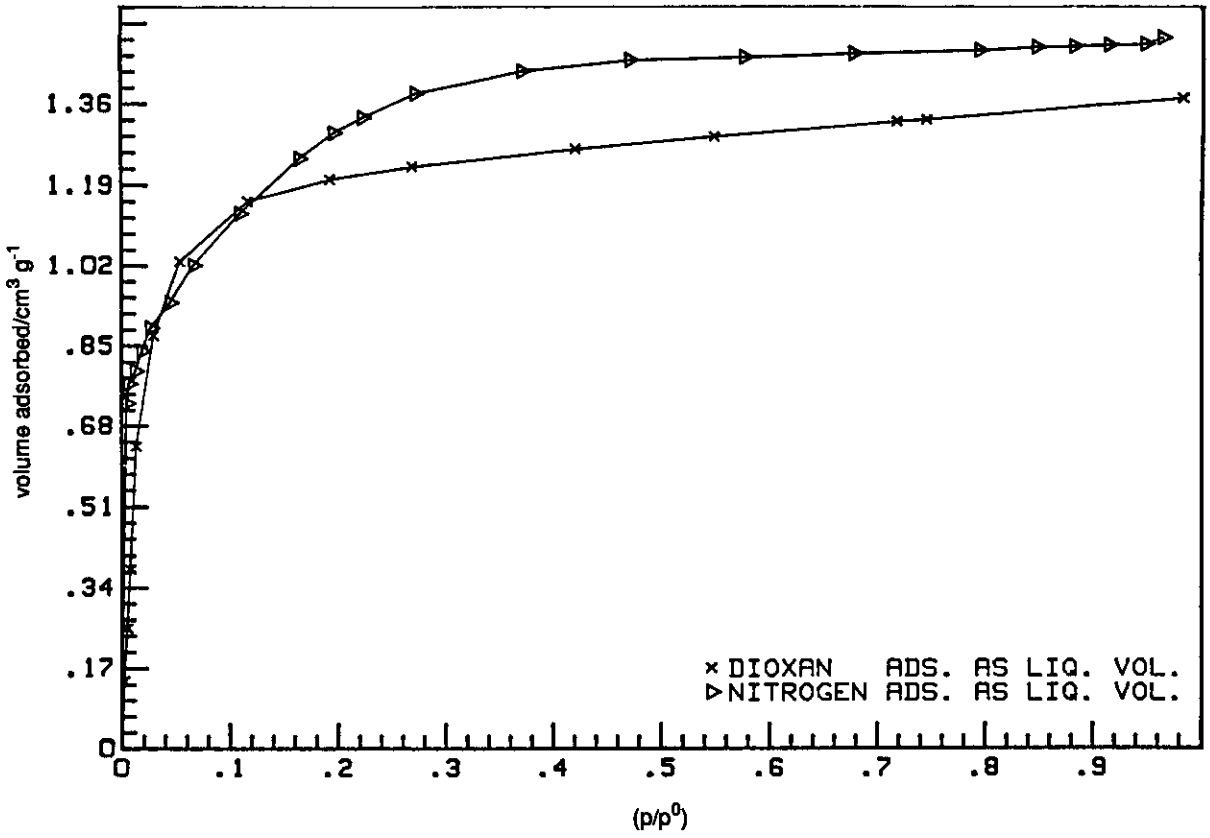

FIG. 10. Comparison of nitrogen and dioxan uptakes by AX21 as liquid volumes.

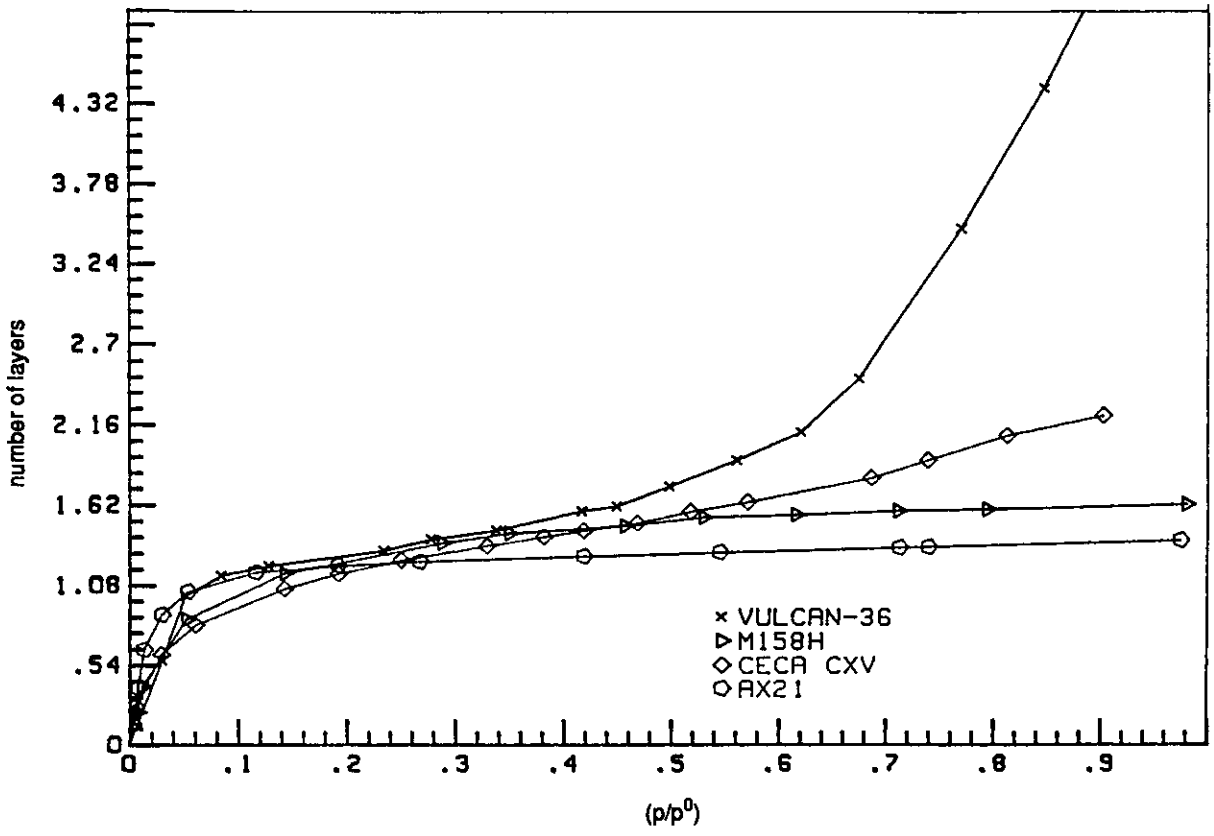

FIG. 11. Isotherms expressed as number of adsorbed layers of dioxan on four carbons.

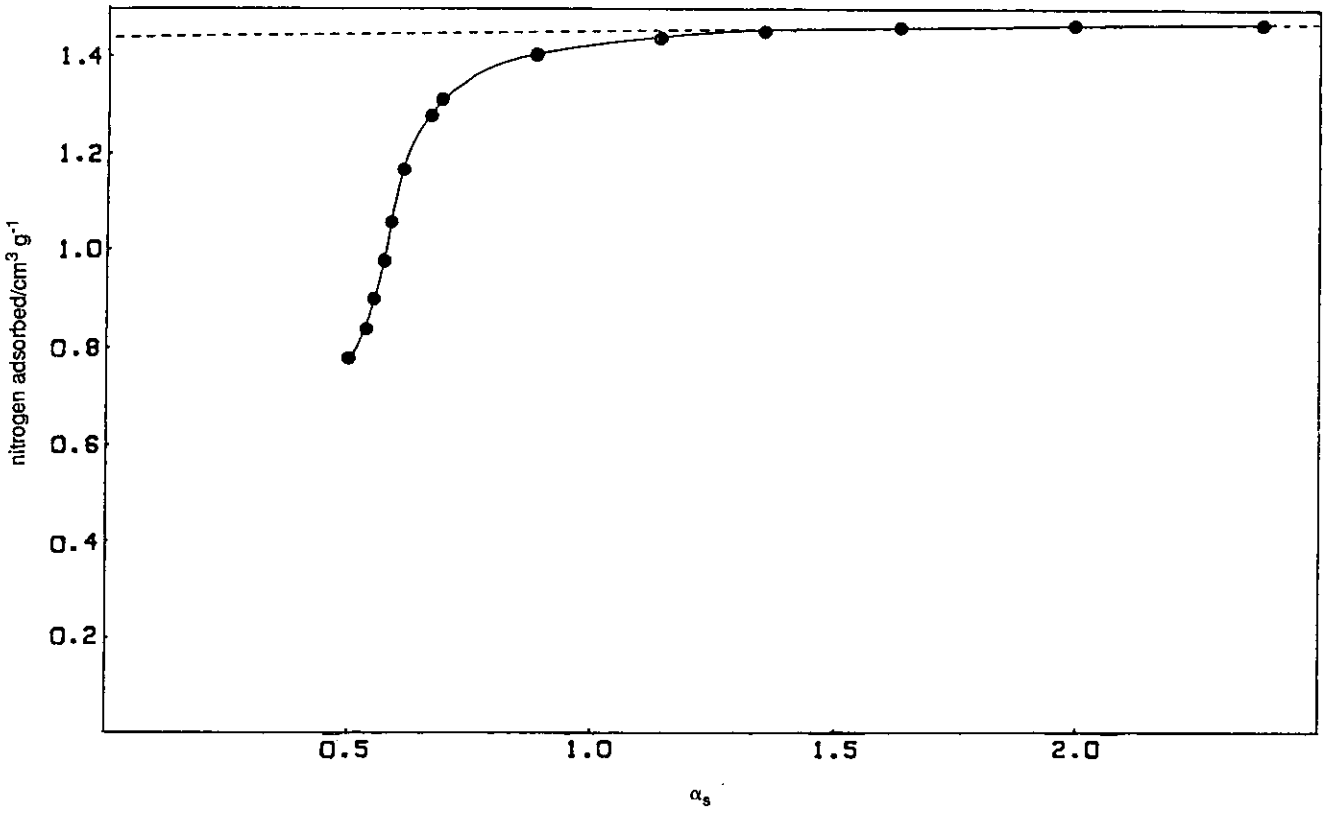

FIG. 12. α_s-plot for nitrogen on AX21.

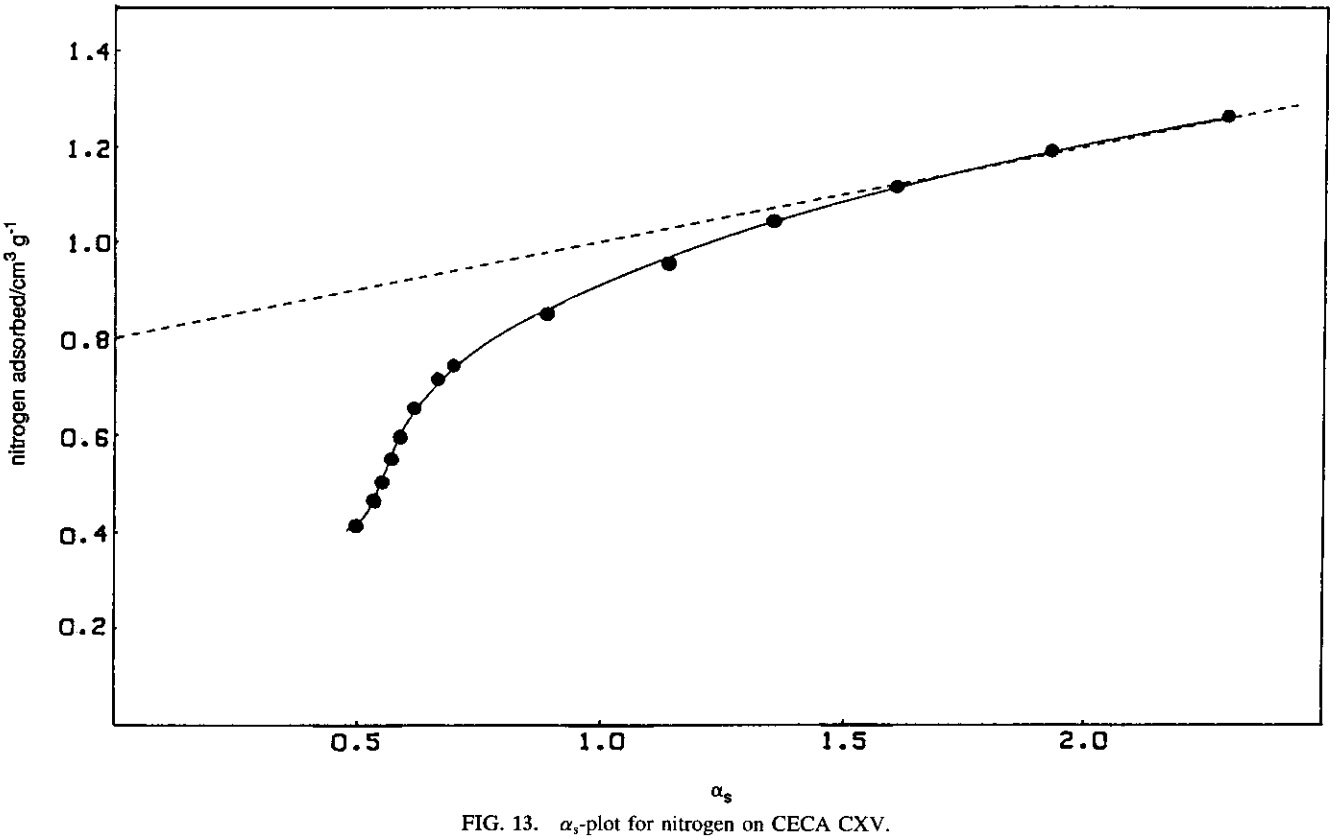

FIG. 13. α_s-plot for nitrogen on CECA CXV.

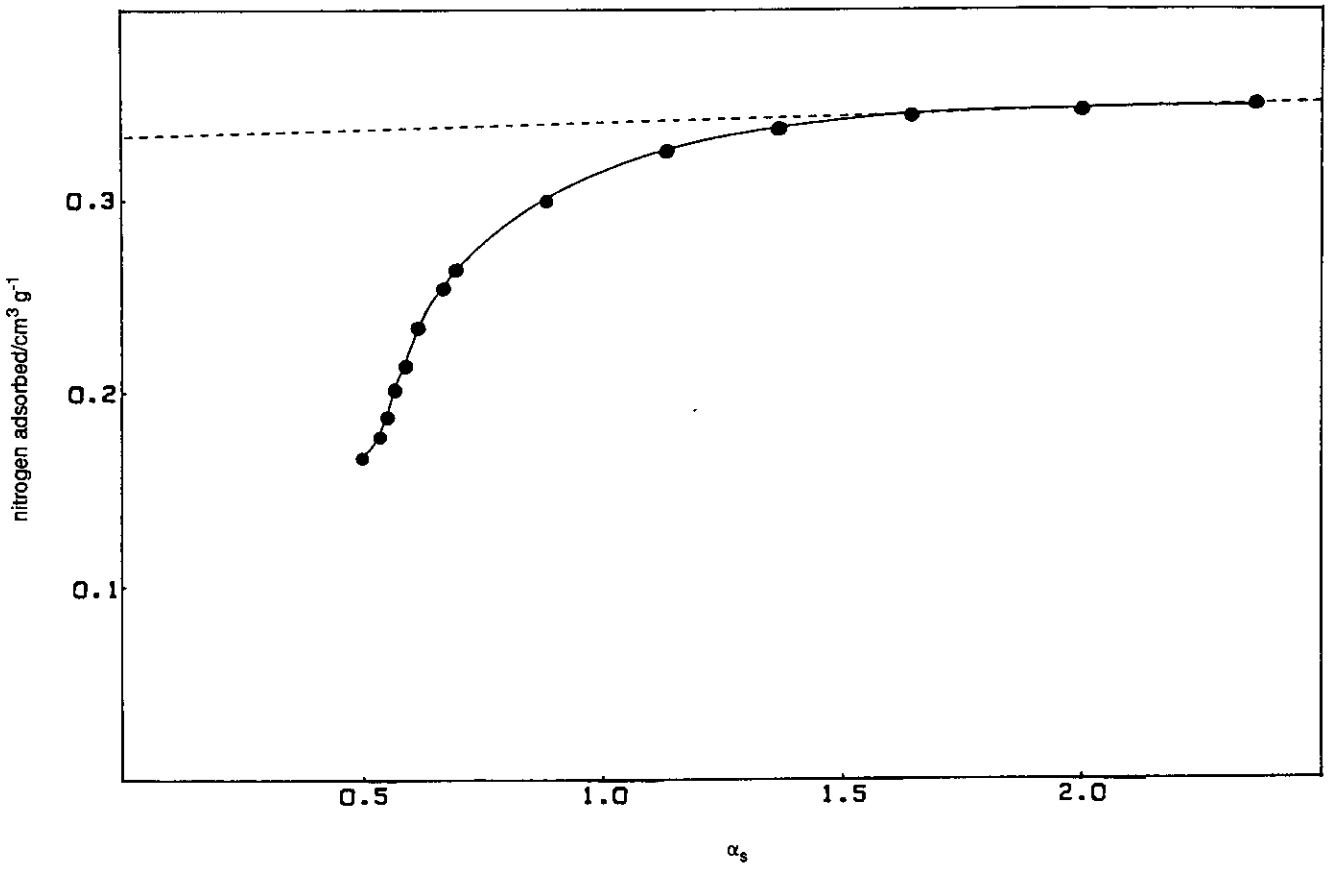

FIG. 14. α_s-plot for nitrogen on M158H.

non is caused by adsorbate molecules forcing their way between primary particles and causing changes in the adsorbent structure which, under normal desorption conditions, prove to be irreversible. The present M158H comprised small hard pellets which resisted crushing and therefore this apparent rigidity would not be consistent with carbon which might undergo structural change induced by adsorbate molecules. A more likely cause of low-pressure hysteresis is the type of activated diffusion process described by Marsh (3). Figure 6 includes the adsorption branch of a dioxan isotherm on 86.11 mg of M158H at 293.2 K, the isotherm for the 60.40-mg sample being recorded at a sample temperature of 293.0 K. The 86.11-mg sample yielded a saturation uptake of 0.370 $cm^3\ g^{-1}$, which as expected for the higher temperature was lower than the value of 0.391 $cm^3\ g^{-1}$ for the 60.40-mg sample. However, the uptake for the higher temperature isotherm was higher than that for the lower temperature at low relative pressures $(p/p^0) < 0.26$. One explanation would be that an activated process occurs in the narrowest pores and therefore at lower temperatures the instrument recording mass change would reach a plateau indicating the apparent attainment of adsorption equilibrium before a very slow process of diffusion of adsorbate through constructions of near molecular dimensions was complete. At higher pressures diffusion becomes faster and a true equilibrium estimate of adsorption is more rapidly attained.

BET analysis of the dioxan isotherm for the 60.40-mg sample gave a surface area of 724 $m^2\ g^{-1}$ which does not agree well with the area of 618 $m^2\ g^{-1}$ from nitrogen adsorption at 77 K. The discrepancy may have arisen because the isotherm points which fall in the BET range did not correspond to true adsorption equilibria. Data at the higher temperature for the 86.11-mg sample gave better agreement with a surface area of 639 $m^2\ g^{-1}$.

CECA CXV. The isotherm for dioxan adsorption on CECA CXV shows an H3-type hysteresis loop (Fig. 7). The similarity between nitrogen and dioxan uptakes, converted to liquid volumes (Fig. 8), suggests that a similar adsorption course occurs for the two adsorbates. The continuous rise in uptakes over the entire pressure range points to the presence of a wide range of both micro- and meso-sized pores. The adsorption capacity of CECA CXV for nitrogen, 1.38 $cm^3\ g^{-1}$ at $(p/p^0) = 0.98$, was slightly greater than that, 1.30 $cm^3\ g^{-1}$ at $(p/p^0) = 0.90$, for dioxan. The nitrogen uptake is greater than that of dioxan below $(p/p^0) = 0.68$ but, unlike the behavior of M158H, there is no pronounced difference in isotherm shape. It can be inferred that the ratio of pore width to adsorbate molecular diameter, which would

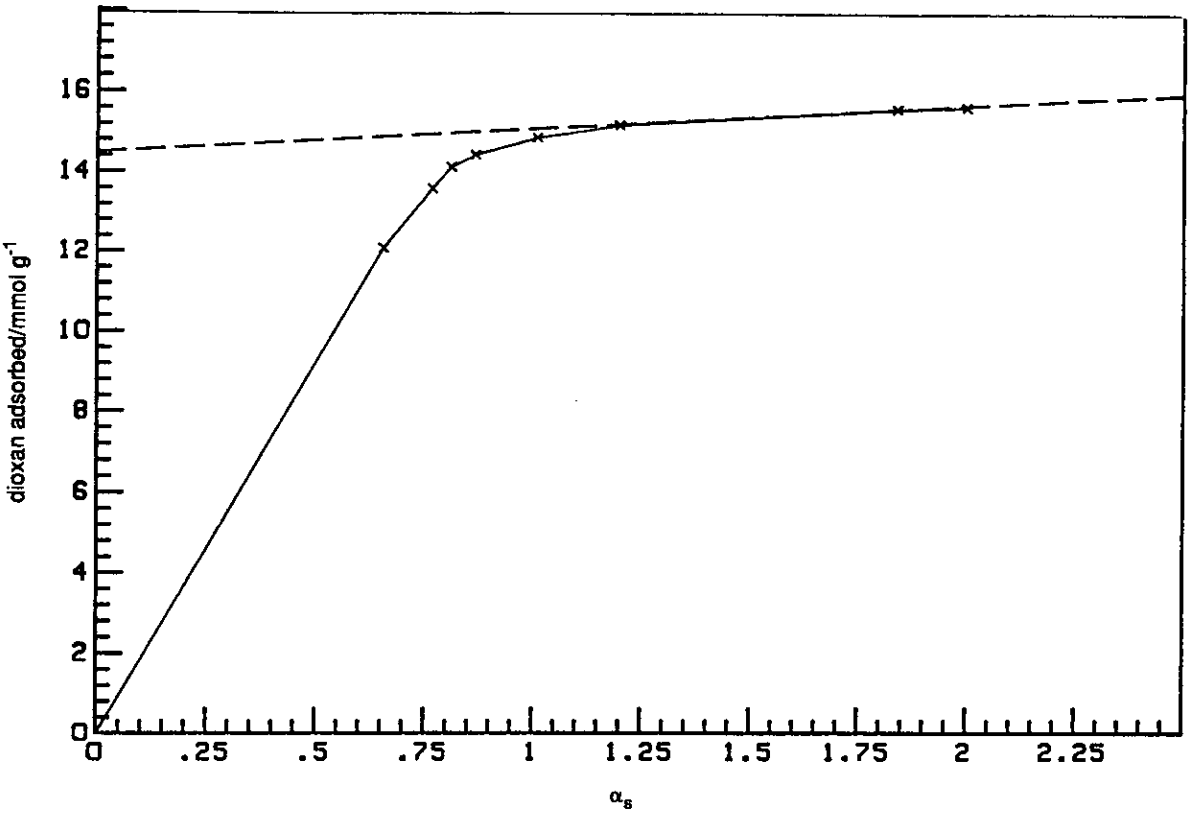

FIG. 15. α_s-plot for dioxan on AX21.

influence adsorption behavior, is not significantly distorted in CECA CXV when changed from nitrogen to dioxan.

BET analysis for dioxan on CECA CXV yields a monolayer capacity of 604.85 mg g^{-1} which is consistent with a surface area of 1753 m^2 g^{-1}, in excellent agreement with the nitrogen adsorption value of 1752 m^2 g^{-1}.

AX21. The isotherm for dioxan adsorption on AX21 was of type I (Fig. 9) and was characterized by the coincidence of the adsorption and desorption branches and the large proportion of the pore volume which is filled at low pressures (50% filled by $(p/p^0) = 0.02$ and 90% by $(p/p^0) = 0.27$).

Comparison of dioxan and nitrogen adsorption on AX21 (Fig. 10) shows that nitrogen adsorption is greater up to $(p/p^0) = 0.03$, dioxan uptake is greater in the short approximate range $0.03 < (p/p^0) < 0.11$, and nitrogen adsorption is again higher at $(p/p^0) > 0.11$. The final dioxan uptake (1.37 cm^3 g^{-1}) is lower than that of nitrogen (1.56 cm^3 g^{-1}). Also the knee of the dioxan isotherm is sharper. This suggests that dioxan only fills a proportion of the micropores which fill with nitrogen at $(p/p^0) < 0.03$. This is followed by a short regime in which dioxan fills pores in which the ratio of pore width to molecular diameter is such that there is enhancement in dioxan adsorption compared with nitrogen adsorption in the same pores. The sharp knee is characteristic of a micropore filling mechanism which has become more primary than secondary. The lower plateau for dioxan rather than nitrogen adsorption suggests that some of the micropores in AX21 are accessible only to nitrogen and not to dioxan molecules.

BET analysis for dioxan on AX21 gave a monolayer capacity of 1028.01 mg g^{-1} and a surface area of 2979 m^2 g^{-1}. This lower value than that of 3098 m^2 g^{-1} from the nitrogen adsorption data provides further evidence that a small proportion of the AX21 surface could not be accessed by dioxan.

BET Surface Areas of Carbons

Very high BET surface area values are of little significance in absolute physical terms. Figure 11 compares dioxan adsorption on the four carbon samples in terms of the number of adsorbed layers, deduced by dividing uptakes by the monolayer BET capacities. The biggest contrast is between nonporous Vulcan-3G which gives a buildup of several layers of dioxan on its surface and microporous AX21 which accommodates an equivalent maximum of 1.4 layers of dioxan. The notion that the entire pore volume of AX21 is filled by dioxan in approximately a monomolecular layer is unrealistic. The rationale for the use of the alternative term monolayer equivalent area lies in the apparent limit imposed by highly microporous solids on the number of adsorbate layers which are allowed to develop. The adsorbate which fills the micropores may be considered capable of covering

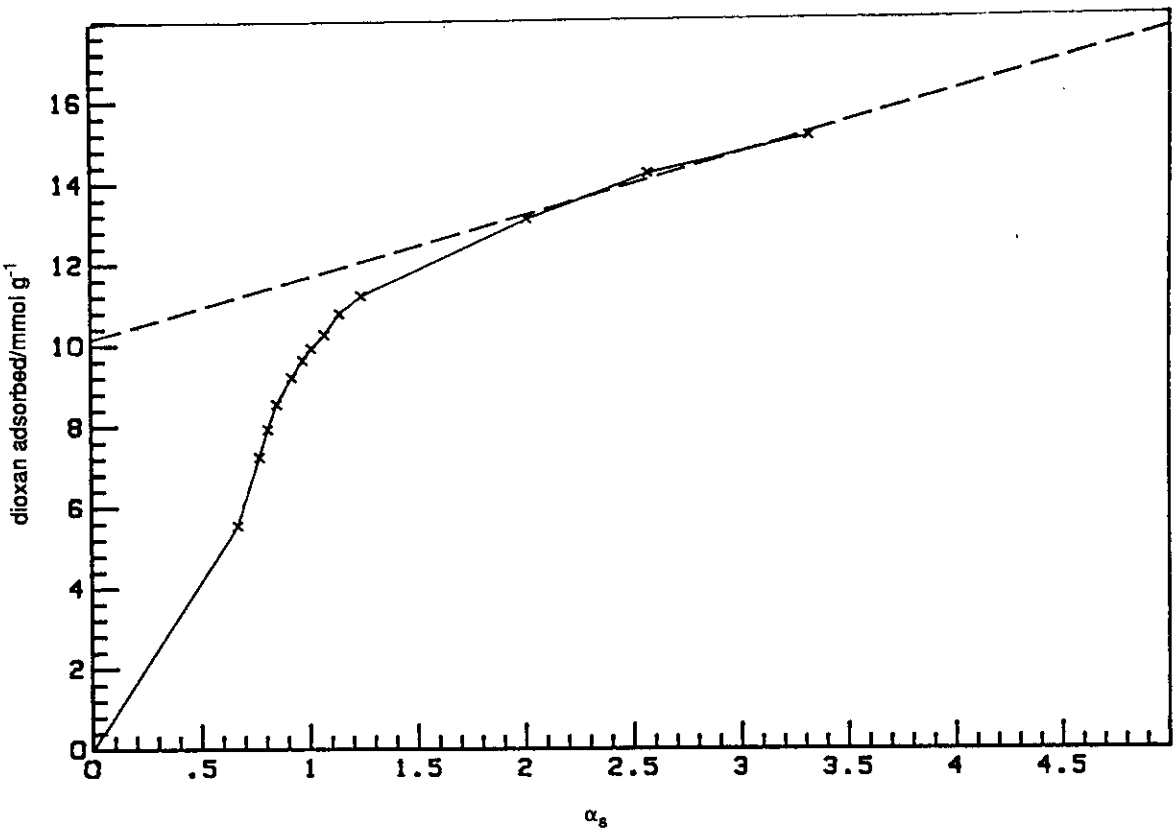

FIG. 16. α_s-plot for dioxan on CECA CXV.

an equivalent area if it were spread as a monomolecular layer. However (16), multilayer adsorption must occur during the filling of micropores in carbons which have large adsorption capacities although not in the exact manner proposed (2) by BET theory.

Any calculation of monolayer capacity is tied to BET theory and hence it is only valid to use BET areas of highly microporous materials for comparative purposes (3). Surface areas of the present porous carbons deduced by BET analysis, with the area occupied per dioxan molecule of 0.424 nm^2 from adsorption results for Vulcan-3G, are as follows:

Carbon sample	N_2 area (m^2 g^{-1})	Dioxan area (m^2 g^{-1})
AX21	3098	2979
CECA CXV	1752	1753
M158H	618	639

The areas derived from the nitrogen and dioxan data show good agreement with a maximum deviation of <4%. There are very few molecules for which a_m, the area occupied per adsorbed molecule, will apply for all adsorbents (17). The tendency of adsorbate molecules to become localized on lattice sites or more active parts of the solid surface implies that the a_m value needed to give a surface area consistent with that derived from nitrogen adsorption data will be a function of the adsorbent. However, the above table suggests that the surfaces of AX21, CECA CXV, and M158H are not significantly different and that the dioxan a_m value calculated from adsorption data for Vulcan-3G is appropriate for use for these three porous carbons. However, the a_m value is valid for these carbons only in that it creates consistency between surface areas derived from nitrogen and dioxan adsorption data. There is no guarantee that the actual area of carbon surface occupied by each adsorbed dioxan molecule is 0.424 nm^2 and the results are subject to the limitations of quoting surface areas for highly porous carbon materials.

The calculation of $a_m = 0.162$ nm^2 for nitrogen from the equation

$$a_m = f(M/pL)^{2/3},$$

in which M is the molecular weight of adsorbate of liquid density p, L is the Avogadro constant, and f is a packing factor equal to 1.091 for spherical shape and hexagonal close packing of the molecules, may be replicated for dioxan. The resulting value of 0.296 nm^2 is too small to give surface areas for the present carbons consistent with the nitrogen adsorption data. However, liquid density calculations for

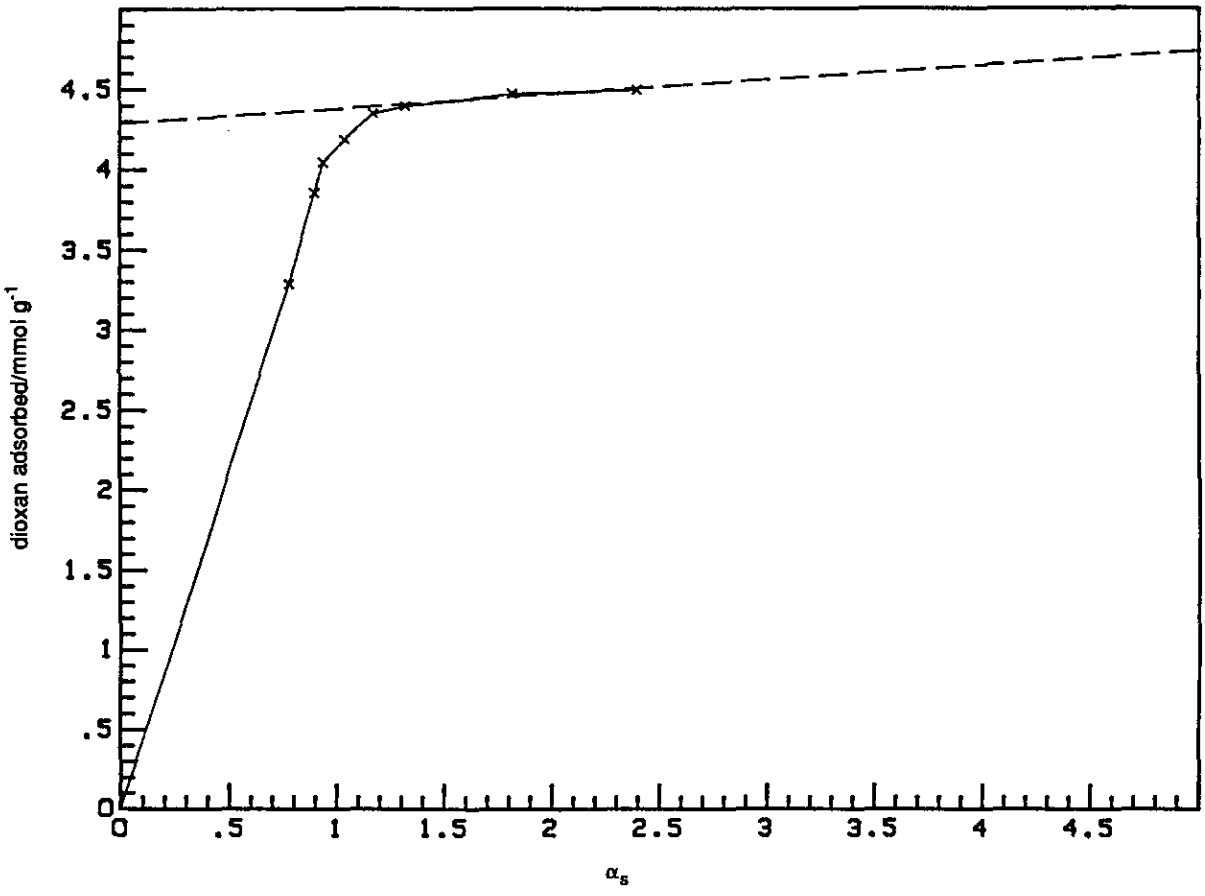

FIG. 17. α_s-plot for dioxan on M158H.

most adsorbates give smaller estimates of a_m than adsorption methods (17) and suffer from the deficiencies that the environment of an adsorbed molecule will differ from that of a molecule in liquid adsorbate and that the assumptions of spherical shape and hexagonal close packing will not be valid, although the assumption of spherical symmetry for a ring compound like dioxan may be less in error than, for example, for a linear alkane. Even for nitrogen a value a_m = 0.20 nm^2 appears to be more appropriate for monolayer coverage of a graphitized carbon surface than the calculated value of 0.162 nm^2 (18, 19). The comparisons of data embodied in Figs. 6, 8, and 10 are not subject to uncertainties associated with assumptions about the specific shape or packing of adsorbate molecules. However, differences between molecular environments in the adsorbed and liquid states remain an uncertainty, although the plots provide a helpful way of comparing data for different adsorbates.

α_s-Plots for Nitrogen Adsorption

An assessment of the dioxan data by the α_s-method (20, 21) benefits from an initial analysis of the nitrogen data by the same method. Despite caution against the use of a single graphitized carbon as a standard (22), Vulcan-3G has been used before in this context (23, 24). The α_s-plots for the three porous carbons are shown in Figs. 12–14 with uptakes expressed as cm^3 of liquid per gram of adsorbent.

For AX21 (Fig. 12) the upturn to the steepest section of the plot above α_s = 0.54 ((p/p^0) = 0.02) and the majority (>90%) of pore filling completed by α_s = 0.7 ((p/p^0) = 0.2) suggest that results in this range may be attributed to secondary micropore filling (25, 26). The upward swing of the α_s-plot suggests that the cooperative mechanism of secondary filling involves an enhancement in adsorption energy. The slight tail at α_s = 0.5 ((p/p^0) = 0.01) corresponds to primary filling of the narrowest micropores in AX21. The near-horizontal plot in the high-pressure region indicates the negligible extent of the external (nonmicropore) surface of AX21. The linear section of the α_s-plot gives a micropore adsorption capacity of 1.44 cm^3 g^{-1} and a monolayer capacity of the mesopores of 1.96 × 10^{-4} mol g^{-1} which corresponds to a surface area of 19 m^2 g^{-1}, equivalent to only 0.6% of the BET surface area for AX21.

For CECA CXV the tail at low pressure (α = 0.5, (p/p^0) = 0.01) leads into a steep section which is indicative of primary followed by secondary micropore filling. However, the end of the steep section corresponds to filling of ca. 55% of capacity (Fig. 13) compared with >90% filling

for AX21 by the same stage. Also the slope of the linear section indicates a much higher mesopore area for CECA CXV than for AX21. Thus the micropore capacity is 0.81 $cm^3\ g^{-1}$ and the mesopore monolayer capacity is 3.26×10^{-3} mol g^{-1}, equivalent to a mesopore surface area of 318 $m^2\ g^{-1}$. The general form of the α_s-plot suggests that a wide range of pore sizes are present in CECA CXV.

The α_s-plot for M158H (Fig. 14) has a near-horizontal section typical of a low mesopore surface area as for AX21, but the low-pressure behavior resembles the result for CECA CXV. Primary followed by secondary pore filling is again exhibited. The linear section gives 0.33 $cm^3\ g^{-1}$ for the micropore capacity and 1.14×10^{-4} mol g^{-1} for the mesopore monolayer capacity which corresponds to a surface area of 11 $m^2\ g^{-1}$ or 1.8% of the total BET surface area.

Secondary filling should occur in wider micropores up to (p/p^0) 0.2–0.3 (24). If it is assumed here that this corresponds to α_s = ca. 0.7 for the completion of secondary filling then at this point AX21 is almost completely filled as a result of primary and secondary micropore filling, M158H has taken up 75% of its capacity, and CECA CXV has taken up only 55% of its capacity but adsorption continues on the relatively large mesopore surface. Of the two samples identified as of mixed type I + IV, M158H is predominantly of type I whereas CECA CXV is more mixed in its porosity.

α_s-Plots for Dioxan Adsorption

The construction of α_s-plots for dioxan adsorption on the three porous carbons (Figs. 15–17) involved the results for dioxan on Vulcan-3G as standard.

For AX21 the linear section of the α_s-plot (Fig. 15) gives an intercept corresponding to a micropore volume of 1.23 $cm^3\ g^{-1}$ which compares with the value of 1.44 $cm^3\ g^{-1}$ from nitrogen adsorption. Nitrogen tends to give higher micropore volumes than other adsorbates (25, 27) either because of a packing factor or because nitrogen can gain access to very narrow pores which exclude other molecules. The difference of 0.21 $cm^3\ g^{-1}$ between the effective pore volumes (27) deduced from nitrogen and dioxan adsorption could be attributable to the volume of pores which allow access to nitrogen molecules (width = ca. 0.3 nm) but exclude dioxan molecules (ca. 0.6 nm). However, the latter dimension is consistent with a plan view orientation of dioxan as envisaged for adsorption of the molecule flat on the surface. This will differ from the end elevation or molecular height. Dioxan may gain access to slit-like micropores by adsorbing end on. A complication is that dioxan can exist as chair or boat conformers. The boat form, despite having the higher energy, represents a more compact molecular form and therefore a chair-to-boat conformational flip may be favored if the energy benefit associated with penetration into a micropore was large enough. The gradient of the linear section of the α_s-plot for AX21 yields a value of 3.54×10^{-4} mol g^{-1} for the external surface monolayer capacity, and hence a surface area of 90 $m^2\ g^{-1}$ which, although larger than the value from nitrogen data, still constitutes only ca. 3% of the total BET surface area.

The α_s-plots for CECA CXV (Fig. 16) and M158H (Fig. 17) give effective micropore volumes a^0_{mi} and mesopore surface areas S_{me} which compare with the data from nitrogen α_s-plots as follows:

	Nitrogen α_2-plot		Dioxan α_s-plot	
Carbon sample	a^0_{mi} ($cm^3\ g^{-1}$)	S_{me} ($m^2\ g^{-1}$)	a^0_{mi} ($cm^3\ g^{-1}$)	S_{me} ($m^2\ g^{-1}$)
AX21	1.44	19	1.23	90
CECA CXV	0.81	318	0.86	260
M158H	0.33	11	0.37	15

The table shows that for CECA CXV or M158H the parameters deduced from dioxan and nitrogen α_s-plots show reasonable agreement. The broad distribution of pore sizes in these two carbons makes it difficult to recognize changes in the adsorption process as a result of the change of adsorbate from nitrogen to dioxan. From the dioxan α_s-plots at $(p/p^0) = 0.2$, for which secondary micropore filling is undoubtedly occurring, the amounts of dioxan adsorbed correspond to a filling percentage of 90% for AX21, 53% for CECA CXV, and 78% for M158H, figures which are compatible with the results for nitrogen at the same relative pressure.

CONCLUSIONS

(a) Nitrogen adsorption data show that the four carbons chosen for study are nonporous (Vulcan-3G), mixed meso- and microporous (CECA CXV), largely microporous with some mesopores (M158H), and highly microporous (AX21).

(b) The general forms of the isotherms for dioxan adsorption on the carbons resembled the corresponding adsorption data for nitrogen although there was slight evidence for steric exclusion of dioxan from some pores accessible to nitrogen and for activated adsorption of dioxan at low relative pressures.

(c) Vulcan-3G is an acceptable standard material giving an average area occupied per adsorbed dioxan molecule of 0.424 nm^2 and hence allowing the determination of surface areas of porous carbons by BET analysis of dioxan adsorption data.

(d) Analysis of dioxan adsorption data by the α_s-plot method gave effective micropore volumes and mesopore surface areas which, particularly for CECA CXV and M158H and to a lesser but not seriously deviating extent for AX21,

were consistent with corresponding results from nitrogen adsorption isotherms.

ACKNOWLEDGMENTS

We thank SERC for a research studentship, BP Research Centre for collaboration through the CASE scheme, and Dr. R. Howes and Dr. T. M. Khong for considerable assistance and advice.

REFERENCES

1. Gregg, S. J., and Sing, K. S. W., "Adsorption, Surface Area, and Porosity," 2nd ed. Academic Press, London, 1982.
2. Brunauer, S., Emmett, P. H., and Teller, E., *J. Am. Chem. Soc.* **60,** 309 (1938).
3. Marsh, H., *Carbon* **25,** 49 (1987).
4. Mikhail, R. S., Brunauer, S., and Bodor, E. E., *J. Colloid Interface Sci.* **26,** 45 (1968).
5. Dubinin, M. M., *in* "Progress in Surface and Membrane Science" (J. F. Danielli, M. D. Rosenberg, and D. A. Cadenhead, Eds.), Vol. 9, p. 1. Academic Press, London, 1975.
6. Dubinin, M. M., *Russian Chem. Rev.* **51,** 605 (1982).
7. Dubinin, M. M., *Carbon* **23,** 373 (1985).
8. Marsh, H., Yan, D. S., O'Grady, T. M., and Wennerberg, A., *Carbon* **22,** 603 (1984).
9. Coetzee, J. F., and Chang, T. H., *Pure Appl. Chem.* **57,** 633 (1985).
10. Brunauer, S., Deming, L. S., Deming, W. E., and Teller, E., *J. Am. Chem. Soc.* **62,** 1723 (1940).
11. Sing, K. S. W., Everett, D. H., Haul, R. A. W., Moscou, L., Pierotti, R. A., Roquerol, J., and Siemieniewska, T., *Pure Appl. Chem.* **57,** 603 (1985).
12. Lippens, B. C., Linsen, B. G., and de Boer, J. H., *J. Catal.* **3,** 32 (1964).
13. Lippens, B. C., and de Boer, J. H., *J. Catal.* **4,** 319 (1965).
14. de Boer, J. H., Lippens, B. C., Linsen, B. G., Broekhoff, J. C. P., van den Heuvel, A., and Osinga, T. J., *J. Colloid Interface Sci.* **21,** 405 (1966).
15. Boblick, T., Fried, V., and Halla, E., "Vapour Pressure of Pure Substances." Elsevier, Amsterdam, 1973.
16. Marsh, H., Crawford, D., O'Grady, T. M., and Wennerberg, A., *Carbon* **20,** 419 (1982).
17. McClellan, A. L., and Harnsberger, H. F., *J. Colloid Interface Sci.* **23,** 577 (1967).
18. Pierce, C., *J. Phys. Chem.* **73,** 813 (1969).
19. Zettlemoyer, A. C., *J. Colloid Interface Sci.* **28,** 343 (1968).
20. Sing, K. S. W., *Chem. Ind. (London),* 1520 (1968).
21. Sing, K. S. W., *in* "Surface Area Determination" (D. H. Everett and R. H. Ottewill, Eds.), p. 25. Butterworth, London, 1970 (Proceedings, International Symposium, 1969).
22. Atkinson, D., McLeod, A. I., and Sing, K. S. W., *J. Chem. Phys.* **81,** 791 (1984).
23. Atkinson, D., McLeod, A. I., Sing, K. S. W., and Capon, A., *Carbon* **20,** 339 (1982).
24. Carrott, P. J. M., Roberts, R. A., and Sing, K. S. W., *Carbon* **25,** 59 (1987).
25. Roberts, R. A., Sing, K. S. W., and Tripathi, V., *Langmuir* **3,** 331 (1987).
26. Rodriguez-Reinoso, F., Garrido, J., Martin-Martinez, J. M., Molina-Sabio, M., and Torregrosa, R., *Carbon* **27,** 23 (1989).
27. Sing, K. S. W., *Carbon* **27,** 5 (1989).